

Hadronic effects on the $X(3872)$ meson abundance in heavy ion collisions

Sungtae Cho¹ and Su Hounng Lee¹

¹*Institute of Physics and Applied Physics, Yonsei University, Seoul 120-749, Korea*

We study the hadronic effects on the $X(3872)$ meson abundance in heavy ion collisions. We evaluate the absorption cross sections of the $X(3872)$ meson by pions and rho mesons in the hadronic stage of heavy ion collisions, and further investigate the variation in the $X(3872)$ meson abundance during the expansion of the hadronic matter for its two possible quantum number states; $J^P = 1^+$ and 2^- . We show that the absorption cross sections and the time evolution of the $X(3872)$ meson abundance are strongly dependent on the structure and quantum number of the $X(3872)$ meson. We thus suggest that studying the abundance of the $X(3872)$ meson in relativistic heavy ion collisions provides a chance to infer its quantum number as well as its structure.

PACS numbers: 14.40.Rt, 25.75.-q, 13.75.Lb

I. INTRODUCTION

Relativistic heavy ion collision experiments have made it possible to study a system of quantum chromodynamic (QCD) matter at very high temperature and density in the laboratory [1–5]. The research on the system of deconfined quarks and gluons, so-called quark-gluon plasma (QGP), has also enabled us to understand the possible phase transition between the hot and dense matter and QGP [6]. Moreover, due to the enormous energies produced in heavy ion collisions, particles that are otherwise hard to find in nature could be produced during the quark-hadron phase transition.

Recently STAR Collaboration reported the observation of an antimatter helium-4 nucleus as well as an antimatter hypernucleus produced at RHIC [7, 8], and also tried to measure the signal of an exotic H dibaryon [9]. As attempts to understand the production of particles of these kinds, there have been many studies focusing on their production yields based on both the statistical model and the coalescence model [10–15]. Moreover, as one of the possible methods to understand the structure of the exotic hadrons, a new approach of studying exotic hadrons in relativistic heavy ion collision experiments has been proposed [10, 11]. There, the relation between the production yields of exotic hadrons and the structure at the moment of their formation has been sought out by considering the production of all proposed possible structures using the coalescence model, and it was found that the production yields of exotic hadron candidates strongly reflect their structures.

The abundance of hadrons evaluated at the chemical freeze-out temperature, however, may change due to the dissociation or the absorption by mostly light mesons such as the pion and the ρ meson in the hadronic medium. The effects from the hadronic interactions on the production of heavy quark mesons have been discussed in many literatures. In order to estimate the possibilities of J/ψ suppression in the hadronic matter, one meson exchange model with the effective Lagrangian has been introduced to evaluate the absorption cross sections with light hadrons [16–19]. A similar approach has been ap-

plied to investigate the time evolution of $D_{s,J}(2317)$ meson abundance in the hadronic matter [20]. In this work we investigate the hadronic medium effects on the production yield of one of exotic mesons, the $X(3872)$ meson.

The $X(3872)$ meson was first discovered by Belle Collaboration [21] from the measurement of $B^+ \rightarrow J/\Psi\pi^+\pi^-K^+$ decay, and later confirmed by CDF [22], D0 [23], and BABAR [24] collaborations. The additional decay modes of $X(3872)$ mesons to $D^0\bar{D}^0\pi^0$ [25–27], $J/\Psi\omega$ [28], $J/\Psi\gamma$ [29], and $\Psi(2s)\gamma$ [30] have also been observed. The positive charge parity of the $X(3872)$ meson has been established by the observation of the $X(3872)$ meson decaying to $J/\Psi\gamma$ [29] and $\Psi(2s)\gamma$ [30], and the current world average mass of the $X(3872)$ meson in PDG [31] is 3871.68 ± 0.17 MeV. However, it is still not clear what the exact structure and quantum number of the $X(3872)$ meson is. Suggested hypotheses for the structure of the $X(3872)$ meson include a pure charmonium state, a \bar{D}^0D^{*0} hadronic molecule, a tetra-quark state, and a charmonium-gluon hybrid state [32]. From the analysis of the angular distribution of the $X(3872)$ meson decaying to $J/\Psi\pi^+\pi^-$ [33], we now understand that the possible quantum number J^P should be either 1^+ or 2^- .

There are various experimental results supporting each spin possibility of the $X(3872)$ meson. The study of the $X(3872)$ meson decaying to \bar{D}^0D^{*0} disfavors the 2^- quantum number because of the angular momentum barrier in its near-threshold decay [25, 26]. On the other hand, the analysis of the $X(3872)$ meson decaying to $J/\Psi\omega$ favors a p wave in the final state, 2^- [28]. We expect that the two different spin possibilities of the $X(3872)$ meson will also lead to different experimental results in heavy ion collision experiment.

After the $X(3872)$ meson is produced at the chemical freeze-out, it interacts with other hadrons during the expansion of the hadronic matter. As a result, the $X(3872)$ meson can be absorbed by the comoving light mesons or additionally produced from interactions between charmed mesons such as D and \bar{D}^* . Evaluating the $X(3872)$ meson cross sections by light hadrons therefore should be useful in estimating the hadronic effects on the $X(3872)$ meson abundance in heavy ion collisions.

However, the $X(3872)$ meson would interact with light hadrons differently depending on the spin of the $X(3872)$ meson. In order for the spin-2 $X(3872)$ meson to interact with light mesons, there should be a charmed meson having the relative momentum to satisfy the angular momentum conservation. Also the spin-2 $X(3872)$ meson should carry a symmetric traceless spin polarization tensor whereas the spin-1 $X(3872)$ meson carries a polarization vector. Therefore, we expect to obtain two different results when we evaluate the cross sections of the $X(3872)$ meson for the two different spin states. By comparing these results with the experimental observation in heavy ion collisions, we may obtain a hint for the quantum number of the $X(3872)$ meson.

In this study we restrict our consideration of the $X(3872)$ meson structure to the spin-1 tetra-quark state and the spin-2 pure charmonium state. We briefly discuss the $\bar{D}^0 D^{*0}$ hadronic molecule for the spin-1 $X(3872)$ meson possibly produced during the hadronic stage and at the kinematical freeze-out point. All the discussion will be focused on the central heavy ion collisions at Relativistic Heavy Ion Collider (RHIC) at Brookhaven National Laboratory; using a model developed to describe the dynamics of the central Au+Au collisions at $\sqrt{s_{NN}} = 200$ GeV. Hereafter, we use simplified notations for the $X(3872)$ meson; X_1 for a 1^+ state and X_2 for a 2^- state.

This paper is organized as follows. In Sec. II, we briefly discuss the production of the $X(3872)$ meson at the chemical freeze-out in both the statistical and coalescence model. Then we consider the interaction of the $X(3872)$ meson with light mesons such as pions and ρ mesons, and evaluate the cross sections of the $X(3872)$ meson in the hadronic medium in Sec. III. In Sec. IV we investigate the time evolution of the $X(3872)$ meson abundance by solving the kinetic equation based on the phenomenological model. Section V is devoted to conclusions. In Appendix A, we discuss the dependence of the strong-coupling constants on the $X(3872)$ meson mass. We briefly address the hadronic effects on the $X(3872)$ meson by baryons in Appendix B.

II. $X(3872)$ MESON PRODUCTION FROM THE QUARK-GLUON PLASMA

We evaluate the production yields of the $X(3872)$ meson in heavy ion collisions using both the statistical and the coalescence model. The statistical model, which assumes that hadrons are in thermal and chemical equilibrium when they are produced at chemical freeze-out in heavy ion collisions, has been very successful in describing the production yields of hadrons [34–37]. We apply the same parameters evaluated in Ref. [11] to obtain the thermal yields.

$$N_X^{\text{stat}} = V_H \frac{g_X}{2\pi^2} \int_0^\infty \frac{p^2 dp}{\gamma_C^{-1} e^{E_X/T_H} \pm 1}$$

$$\approx \frac{\gamma_C g_X V_H}{2\pi^2} m_X^2 T_H K_2(m_X/T_H), \quad (1)$$

where the Maxwell-Boltzmann approximation has been made in the second line. We consider the $X(3872)$ meson produced at the hadronization temperature $T_H = 175$ MeV when the volume of the quark-gluon plasma, V_H is 1908 fm^3 [10, 11]. We assume that the total number of charm quark produced from the initial hard collisions at RHIC is 3, which leads to the charm quark fugacity factor $\gamma_C = 6.4$ by the requirement that the charm quark is conserved among charmed hadrons such as D , D^* , D_s mesons, and Λ_c . The difference in the yields between the spin-1 $X(3872)$ meson and the spin-2 $X(3872)$ meson originates only from the spin degeneracy g_X in the statistical model.

In the coalescence model, which successfully explains both the enhancement of the baryon to meson ratio in the intermediate transverse momentum region [38–41] and the quark number scaling of the elliptic flows [42], we consider the yields of the $X(3872)$ meson produced from both the four quark configuration for the spin-1 state and the two quark configuration for the spin-2 state. We assume that the quark coalescence occurs in the volume 1000 fm^3 and the mass of light constituent quarks is 300 MeV, while that of a charm constituent quark is 1500 MeV. We also assume that the available light quark number at hadronization temperature is 245. We adopt the oscillator frequency of the Wigner function for charmed hadrons $\omega_c = 385$ MeV obtained by requiring that the coalescence model reproduces well the yield of $\Lambda_c(2286)$ in the statistical model. For details, refer to Ref. [11]. We summarize the production yields of the $X(3872)$ meson in Table I.

TABLE I: The $X(3872)$ meson yields in central Au+Au collisions at $\sqrt{s_{NN}} = 200$ GeV at RHIC in both the statistical and coalescence model. The yields for the spin-2 state differ from those in Table V. of Ref. [11] by the spin degeneracy factor 5/3.

$X(3872)$	Coal.(2q)	Coal.(4q)	Stat.
spin-1		4.0×10^{-5}	2.9×10^{-4}
spin-2	1.7×10^{-4}		4.8×10^{-4}

In Table I, the smaller yields in the coalescence model compared to those in the statistical model reflect the suppression effects in the quark coalescence process. The suppression mechanism is, however, different for different spin states of the $X(3872)$ meson. The coalescence of additional quarks to construct the tetraquark state makes the yield suppressed for the spin-1 $X(3872)$ meson whereas the construction of a d -wave coalescence factor leads to the smaller yield for the spin-2 $X(3872)$ meson.

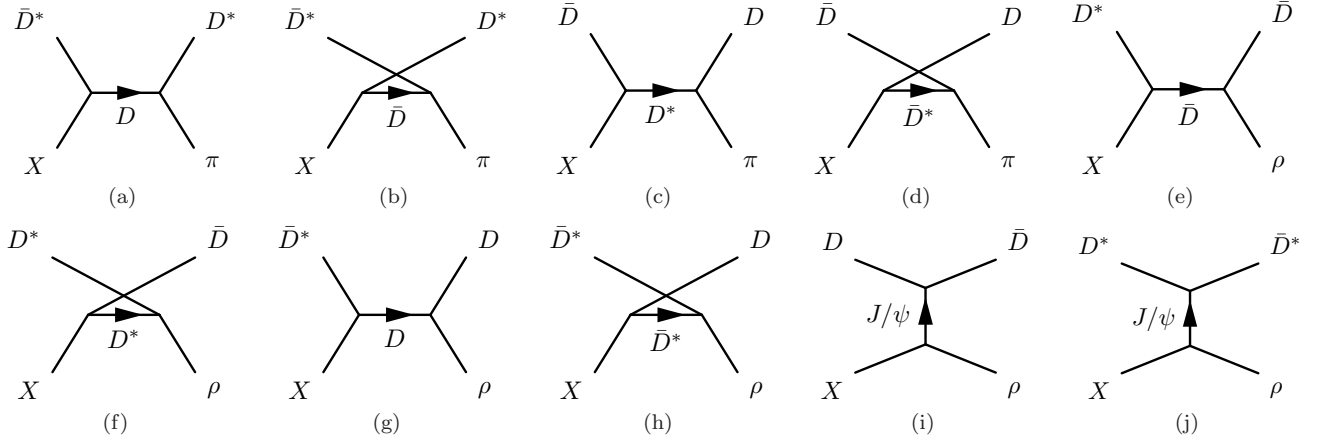


FIG. 1: Born diagrams for $X(3872)$ absorption by pions and ρ mesons: $X\pi \rightarrow \bar{D}^* D^*$, (a) and (b); $X\pi \rightarrow \bar{D} D$, (c) and (d); $X\rho \rightarrow D^* \bar{D}$, (e) and (f); $X\rho \rightarrow \bar{D}^* D$, (g) and (h); $X\rho \rightarrow D \bar{D}$, (i); and $X\rho \rightarrow D^* \bar{D}^*$, (j).

III. HADRONIC EFFECTS ON THE $X(3872)$ MESON

The $X(3872)$ meson produced at the chemical freeze-out interacts with other hadrons during the expansion of the hadronic matter. As a result the $X(3872)$ meson can be absorbed by the comoving light mesons or produced from the interaction between charmed mesons such as D and \bar{D}^* . We consider here the $X(3872)$ meson interacting with light mesons such as pions and ρ mesons,

$$\begin{aligned} X\pi &\rightarrow \bar{D}^* D^*, & X\pi &\rightarrow \bar{D} D, & X\rho &\rightarrow \bar{D}^* D, \\ X\rho &\rightarrow D^* \bar{D}, & X\rho &\rightarrow D \bar{D}, & X\rho &\rightarrow D^* \bar{D}^*. \end{aligned} \quad (2)$$

The diagrams representing each process in Eq. (2) are shown in Fig. 1. To evaluate the cross sections for these diagrams in Fig. 1, we consider the following interaction Lagrangians

$$\begin{aligned} \mathcal{L}_{\pi DD^*} &= ig_{\pi DD^*} D^{*\mu} \vec{\tau} \cdot (\bar{D} \partial_\mu \vec{\pi} - \partial_\mu \bar{D} \vec{\pi}) + \text{H.c.}, \\ \mathcal{L}_{\rho DD} &= ig_{\rho DD} (D \vec{\tau} \partial_\mu \bar{D} - \partial_\mu D \vec{\tau} \bar{D}) \cdot \vec{\rho}^\mu, \\ \mathcal{L}_{\rho D^* D^*} &= ig_{\rho D^* D^*} [(\partial_\mu D^{*\nu} \vec{\tau} \bar{D}_\nu^* - D^{*\nu} \vec{\tau} \partial_\mu \bar{D}_\nu^*) \cdot \vec{\rho}^\mu \\ &\quad + (D^{*\nu} \vec{\tau} \cdot \partial_\mu \vec{\rho}_\nu - \partial_\mu D^{*\nu} \vec{\tau} \cdot \vec{\rho}_\nu) \bar{D}^{*\mu} \\ &\quad + D^{*\mu} (\vec{\tau} \cdot \vec{\rho}^\nu \partial_\mu \bar{D}_\nu^* - \vec{\tau} \cdot \partial_\mu \vec{\rho}^\nu \bar{D}_\nu^*)], \\ \mathcal{L}_{\psi DD} &= ig_{\psi DD} \psi^\mu (D \partial_\mu \bar{D} - \partial_\mu D \bar{D}), \\ \mathcal{L}_{\psi D^* D^*} &= ig_{\psi D^* D^*} [\psi^\mu (\partial_\mu D^{*\nu} \bar{D}_\nu^* - D^{*\nu} \partial_\mu \bar{D}_\nu^*) \\ &\quad + (\partial_\mu \psi^\nu \bar{D}_\nu^* - \psi^\nu \partial_\mu \bar{D}_\nu^*) \bar{D}^{*\mu} \\ &\quad + D^{*\mu} (\psi^\nu \partial_\mu \bar{D}_\nu^* - \partial_\mu \psi^\nu \bar{D}_\nu^*)]. \end{aligned} \quad (3)$$

In Eq. (3), $\vec{\tau}$ are the Pauli matrices, and $\vec{\pi}$ and $\vec{\rho}$ denote the pion and rho meson isospin triplets, respectively, while $D \equiv (D^0, D^+)$ and $D^* \equiv (D^{*0}, D^{*+})$ denote the pseudoscalar and vector charm meson doublets, respectively. Here the shorthand notation ψ has been used for

the J/ψ meson. These interaction Lagrangians have been obtained from the free Lagrangians for pseudoscalar and vector mesons by introducing the minimal substitution [18]. On the other hand, the interaction Lagrangians for the $X(3872)$ meson have been built to produce strong transition matrix elements for the $X(3872)$ meson decays; $X \rightarrow J/\psi$ and $X \rightarrow D^0 \bar{D}^{*0}$ [43],

$$\begin{aligned} \mathcal{L}_{X_1 D^* D} &= g_{X_1 D^* D} X_1^\mu \bar{D}_\mu^* D, \\ \mathcal{L}_{X_1 \psi \rho} &= ig_{X_1 \psi \rho} \epsilon^{\mu\nu\rho\sigma} \psi_\nu \rho_\rho \partial_\sigma X_{1\mu}, \\ \mathcal{L}_{X_2 D^* D} &= -ig_{X_2 D^* D} X_2^{\mu\nu} \bar{D}_\mu^* \partial_\nu D, \\ \mathcal{L}_{X_2 \psi \rho} &= -g_{X_2 \psi \rho} \epsilon^{\mu\nu\rho\sigma} X_{2\mu\alpha} (\partial_\nu \psi^\alpha \partial_\rho \rho_\sigma - \partial_\nu \rho^\alpha \partial_\rho \psi_\sigma) \\ &\quad + g'_{X_2 \psi \rho} \epsilon^{\mu\nu\rho\sigma} \partial_\nu X_{2\mu\alpha} (\partial^\alpha \psi_\rho \rho_\sigma - \psi_\rho \partial^\alpha \rho_\sigma). \end{aligned} \quad (4)$$

As we see in Eq. (4), we need an additional derivative for the interaction Lagrangians of the spin-2 $X(3872)$ meson compared to those of the spin-1 $X(3872)$ meson to satisfy the angular momentum conservation. The structure of these Lagrangians is expected to make the energy dependence on the cross sections different in the hadronic medium. This is also the factor prohibiting the spin-2 $X(3872)$ meson from decaying to the vector meson D^* and the pseudoscalar meson D near the threshold energy. We need an anti-symmetric tensor $\epsilon^{\mu\nu\rho\sigma}$ to describe the isospin violating interaction between one axial vector meson and two vector mesons for the spin-1 $X(3872)$ meson. This term becomes more complicated for the spin-2 $X(3872)$ meson since the anti-symmetric tensor $\epsilon^{\mu\nu\rho\sigma}$ should not be fully contracted with the symmetric polarization tensor $\pi_{\mu\nu}$.

Based on the above effective Lagrangians, we consider the reactions for the $X(3872)$ meson absorption by pions and ρ mesons shown in Fig. 1. Among those diagrams in Fig. 1 the process $X\rho \rightarrow \bar{D}^* D$ leads to the same cross section as the process $X\rho \rightarrow D^* \bar{D}$. The amplitudes for all processes, without isospin factors and before summing

and averaging over external spins, are represented by

$$\begin{aligned}
\mathcal{M}_{X\pi\rightarrow\bar{D}^*D^*} &\equiv \mathcal{M}_X^{(a)} + \mathcal{M}_X^{(b)}, \\
\mathcal{M}_{X\pi\rightarrow\bar{D}D} &\equiv \mathcal{M}_X^{(c)} + \mathcal{M}_X^{(d)}, \\
\mathcal{M}_{X\rho\rightarrow D^*\bar{D}} &\equiv \mathcal{M}_X^{(e)} + \mathcal{M}_X^{(f)}, \\
\mathcal{M}_{X\rho\rightarrow\bar{D}^*D} &\equiv \mathcal{M}_X^{(g)} + \mathcal{M}_X^{(h)}, \\
\mathcal{M}_{X\rho\rightarrow D\bar{D}} &\equiv \mathcal{M}_X^{(i)}, \\
\mathcal{M}_{X\rho\rightarrow D^*\bar{D}^*} &\equiv \mathcal{M}_X^{(j)},
\end{aligned} \tag{5}$$

where the amplitudes for the first process $X\pi \rightarrow \bar{D}^*D^*$ are

$$\begin{aligned}
\mathcal{M}_{X_1}^{(a)} &= -g_{\pi D^*D}g_{X_1D^*D}\epsilon_1^\mu\epsilon_2^\nu\epsilon_{3\mu}^*\frac{1}{t-m_D^2}(2p_2-p_4)_\nu, \\
\mathcal{M}_{X_1}^{(b)} &= -g_{\pi D^*D}g_{X_1D^*D}\epsilon_1^\mu\epsilon_2^\nu\epsilon_{3\mu}^*\frac{1}{u-m_D^2}(2p_2-p_3)_\nu
\end{aligned} \tag{6}$$

for the spin-1 $X(3872)$ meson and

$$\begin{aligned}
\mathcal{M}_{X_2}^{(a)} &= g_{\pi D^*D}g_{X_2D^*D}\pi_1^{\mu\alpha}\epsilon_2^\nu\epsilon_{3\mu}^* \\
&\quad \times \frac{1}{t-m_D^2}(p_4-p_2)_\alpha(2p_2-p_4)_\nu, \\
\mathcal{M}_{X_2}^{(b)} &= -g_{\pi D^*D}g_{X_2D^*D}\pi_1^{\mu\alpha}\epsilon_2^\nu\epsilon_{3\mu}^* \\
&\quad \times \frac{1}{u-m_D^2}(p_3-p_2)_\alpha(2p_2-p_3)_\nu
\end{aligned} \tag{7}$$

for the spin-2 $X(3872)$ meson. Similarly, the amplitudes for the second process $X\pi \rightarrow \bar{D}D$ are

$$\begin{aligned}
\mathcal{M}_{X_1}^{(c)} &= g_{\pi D^*D}g_{X_1D^*D}\epsilon_1^\mu\frac{1}{t-m_{D^*}^2}(p_2+p_4)^\nu \\
&\quad \times \left(-g_{\mu\nu} + \frac{(p_1-p_3)_\mu(p_1-p_3)_\nu}{m_{D^*}^2}\right), \\
\mathcal{M}_{X_1}^{(d)} &= -g_{\pi D^*D}g_{X_1D^*D}\epsilon_1^\mu\frac{1}{u-m_{D^*}^2}(p_2+p_3)^\nu \\
&\quad \times \left(-g_{\mu\nu} + \frac{(p_1-p_4)_\mu(p_1-p_4)_\nu}{m_{D^*}^2}\right)
\end{aligned} \tag{8}$$

and

$$\begin{aligned}
\mathcal{M}_{X_2}^{(c)} &= -g_{\pi D^*D}g_{X_2D^*D}\pi_1^{\mu\alpha}\frac{1}{t-m_{D^*}^2}(p_2+p_4)^\nu p_{3\alpha} \\
&\quad \times \left(-g_{\mu\nu} + \frac{(p_1-p_3)_\mu(p_1-p_3)_\nu}{m_{D^*}^2}\right), \\
\mathcal{M}_{X_2}^{(d)} &= g_{\pi D^*D}g_{X_2D^*D}\pi_1^{\mu\alpha}\frac{1}{u-m_{D^*}^2}(p_2+p_3)^\nu p_{4\alpha} \\
&\quad \times \left(-g_{\mu\nu} + \frac{(p_1-p_4)_\mu(p_1-p_4)_\nu}{m_{D^*}^2}\right)
\end{aligned} \tag{9}$$

for the 1^+ state and the 2^- state, respectively. And the amplitudes for the process $X\rho \rightarrow \bar{D}^*D$ are

$$\begin{aligned}
\mathcal{M}_{X_1}^{(g)} &= -g_{\rho DD}g_{X_1D^*D}\epsilon_1^\mu\epsilon_2^\nu\epsilon_{3\mu}^*\frac{1}{t-m_D^2}(2p_4-p_2)_\nu, \\
\mathcal{M}_{X_1}^{(h)} &= -g_{\rho D^*D^*}g_{X_1D^*D}\epsilon_1^\mu\epsilon_2^\alpha\epsilon_3^{*\beta}\frac{1}{u-m_{D^*}^2} \\
&\quad \times \left(-g_{\mu\nu} + \frac{(p_1-p_4)_\mu(p_1-p_4)_\nu}{m_{D^*}^2}\right) \\
&\quad \times \left((2p_3-p_2)_\alpha g_\beta^\nu - (p_3+p_2)^\nu g_{\alpha\beta} + (2p_2-p_3)_\beta g_\alpha^\nu\right)
\end{aligned} \tag{10}$$

and

$$\begin{aligned}
\mathcal{M}_{X_2}^{(g)} &= -g_{\rho DD}g_{X_2D^*D}\pi_1^{\mu\gamma}\epsilon_2^\nu\epsilon_{3\mu}^* \\
&\quad \times \frac{1}{t-m_D^2}(2p_4-p_2)_\nu(p_1-p_3)_\gamma, \\
\mathcal{M}_{X_2}^{(h)} &= -g_{\rho D^*D^*}g_{X_2D^*D}\pi_1^{\mu\gamma}\epsilon_2^\alpha\epsilon_3^{*\beta}\frac{1}{u-m_{D^*}^2}p_{4\gamma} \\
&\quad \times \left(-g_{\mu\nu} + \frac{(p_1-p_4)_\mu(p_1-p_4)_\nu}{m_{D^*}^2}\right) \\
&\quad \times \left((2p_3-p_2)_\alpha g_\beta^\nu - (p_3+p_2)^\nu g_{\alpha\beta} + (2p_2-p_3)_\beta g_\alpha^\nu\right).
\end{aligned} \tag{11}$$

Finally the amplitudes for the processes $X\rho \rightarrow D\bar{D}$ and $X\rho \rightarrow D^*\bar{D}^*$ are

$$\begin{aligned}
\mathcal{M}_{X_1}^{(i)} &= g_{\psi DD}g_{X_1\psi\rho}\epsilon^{\mu\nu\rho\sigma}\epsilon_{1\mu}\epsilon_{2\rho}\frac{1}{s-m_\psi^2}(p_4-p_3)_\alpha p_{1\sigma} \\
&\quad \times \left(-g_\nu^\alpha + \frac{(p_1+p_2)_\nu(p_1+p_2)^\alpha}{m_\psi^2}\right) \\
\mathcal{M}_{X_2}^{(i)} &= -g_{\psi DD}g_{X_2\psi\rho}\epsilon^{\mu\nu\rho\sigma}\pi_{1\mu\alpha}\epsilon_{2\sigma}\frac{1}{s-m_\psi^2}(p_4-p_3)_\beta \\
&\quad \times (p_1+p_2)_\nu p_{2\rho} \left(-g^{\alpha\beta} + \frac{(p_1+p_2)^\alpha(p_1+p_2)^\beta}{m_\psi^2}\right) \\
&\quad + g_{\psi DD}g_{X_2\psi\rho}\epsilon^{\mu\nu\rho\sigma}\pi_{1\mu\alpha}\epsilon_2^\alpha\frac{1}{s-m_\psi^2}(p_4-p_3)_\beta \\
&\quad \times (p_1+p_2)_\rho p_{2\nu} \left(-g_\sigma^\beta + \frac{(p_1+p_2)_\sigma(p_1+p_2)^\beta}{m_\psi^2}\right) \\
&\quad + g_{\psi DD}g'_{X_2\psi\rho}\epsilon^{\mu\nu\rho\sigma}\pi_{1\mu\alpha}\epsilon_{2\sigma}\frac{1}{s-m_\psi^2}(p_4-p_3)_\beta \\
&\quad \times (p_1+2p_2)^\alpha p_{1\nu} \left(-g_\rho^\beta + \frac{(p_1+p_2)_\rho(p_1+p_2)^\beta}{m_\psi^2}\right),
\end{aligned} \tag{12}$$

and

$$\mathcal{M}_{X_1}^{(j)} = g_{\psi D^*D^*}g_{X_1\psi\rho}\epsilon^{\mu\nu\rho\sigma}\epsilon_{1\mu}\epsilon_{2\rho}\epsilon_3^*\epsilon_{4\beta}^*\frac{1}{s-m_\psi^2}p_{1\sigma}$$

$$\begin{aligned}
& \times \left((p_3 - p_4)_\alpha g^{\gamma\beta} - (2p_3 + p_4)^\beta g_\alpha^\gamma + (p_3 + 2p_4)^\gamma g_\alpha^\beta \right) \\
& \times \left(-g_\nu^\alpha + \frac{(p_1 + p_2)_\nu (p_1 + p_2)^\alpha}{m_\psi^2} \right) \\
\mathcal{M}_{X_2}^{(j)} = & g_{\psi D^* D^*} \varepsilon^{\mu\nu\rho\sigma} \pi_{1\mu\alpha} \varepsilon_{3\gamma}^* \varepsilon_{4\delta}^* \frac{1}{s - m_\psi^2} \\
& \times \left((p_3 - p_4)_\beta g^{\gamma\delta} - (2p_3 + p_4)^\delta g_\beta^\gamma + (p_3 + 2p_4)^\gamma g_\beta^\delta \right) \\
& \times \left[-g_{X_2\psi\rho} \varepsilon_{2\sigma} \left(-g^{\alpha\beta} + \frac{(p_1 + p_2)^\alpha (p_1 + p_2)^\beta}{m_\psi^2} \right) \right. \\
& \times (p_1 + p_2)_\nu p_{2\rho} + g_{X_2\psi\rho} \varepsilon_2^\alpha (p_1 + p_2)_\rho p_{2\nu} \\
& \times \left(-g_\sigma^\beta + \frac{(p_1 + p_2)_\sigma (p_1 + p_2)^\beta}{m_\psi^2} \right) + g'_{X_2\psi\rho} \varepsilon_{2\sigma} \\
& \left. \times (p_1 + 2p_2)^\alpha p_{1\nu} \left(-g_\rho^\beta + \frac{(p_1 + p_2)_\rho (p_1 + p_2)^\beta}{m_\psi^2} \right) \right], \quad (13)
\end{aligned}$$

respectively, for both the $X_1(3872)$ meson and the $X_2(3872)$ meson.

In the above equations, p_j denotes the momentum of particle j . We choose the convention that particles 1 and 2 represent initial-state mesons, while particles 3 and 4 represent final-state mesons on the left and right sides of the diagrams, respectively. Here we use the usual Mandelstam variables given by $s = (p_1 + p_2)^2$, $t = (p_1 - p_3)^2$, and $u = (p_1 - p_4)^2$. The polarization tensor $\pi^{\mu\nu}$ satisfies the following polarization sum:

$$\begin{aligned}
& \sum_{pol} \pi^{\mu\nu} \pi^{*\mu'\nu'} \\
& = \frac{1}{2} \left(-g^{\mu\mu'} + \frac{k^\mu k^{\mu'}}{m_X^2} \right) \left(-g^{\nu\nu'} + \frac{k^\nu k^{\nu'}}{m_X^2} \right) \\
& + \frac{1}{2} \left(-g^{\mu\nu'} + \frac{k^\mu k^{\nu'}}{m_X^2} \right) \left(-g^{\mu'\nu} + \frac{k^{\mu'} k^\nu}{m_X^2} \right) \\
& - \frac{1}{3} \left(-g^{\mu\nu} + \frac{k^\mu k^\nu}{m_X^2} \right) \left(-g^{\mu'\nu'} + \frac{k^{\mu'} k^{\nu'}}{m_X^2} \right) \\
& = \frac{1}{2} \left(g^{\mu\mu'} g^{\nu\nu'} + g^{\mu\nu'} g^{\mu'\nu} - g^{\mu\nu} g^{\mu'\nu'} \right) - \frac{1}{2m_X^2} \\
& \times \left(g^{\mu\mu'} k^\nu k^{\nu'} + g^{\nu\nu'} k^\mu k^{\mu'} + g^{\mu\nu'} k^{\mu'} k^\nu + g^{\mu'\nu} k^\mu k^{\nu'} \right) \\
& + \frac{1}{6} \left(g^{\mu\nu} + \frac{2}{m_X^2} k^\mu k^\nu \right) \left(g^{\mu'\nu'} + \frac{2}{m_X^2} k^{\mu'} k^{\nu'} \right). \quad (14)
\end{aligned}$$

In obtaining the full amplitudes we introduce the following form factors at interaction vertices to prevent the artificial growth of the tree-level amplitudes with the energy:

$$F(\vec{q}) = \frac{\Lambda^2}{\Lambda^2 + \vec{q}^2}, \quad (15)$$

where \vec{q}^2 is the squared three-momentum transfer for t and u channels and the squared three-momentum of the

incoming particles for s channel taken in the center-of-mass frame. For the cutoff parameter Λ , we use $\Lambda = 2.0$ GeV. The final isospin- and spin-averaged cross section is given by

$$\sigma = \frac{1}{64\pi^2 s g_1 g_2} \frac{|\vec{p}_f|}{|\vec{p}_i|} \int d\Omega |\overline{\mathcal{M}}|^2 F^4, \quad (16)$$

with g_1 and g_2 being the degeneracy factors of the initial 1 and 2 particles, $(2I_1 + 1)(2S_1 + 1)$ and $(2I_2 + 1)(2S_2 + 1)$, respectively. We denote by $|\overline{\mathcal{M}}|^2$ the squared amplitude of all processes in Eq. (5) obtained by summing over the isospins and spins of both the initial and final particles after killing all unphysical terms satisfying $p_{1\mu} \pi_1^{\mu\nu} = 0$, $p_{2\mu} \varepsilon_2^\mu = 0$ and so on. In evaluating $|\overline{\mathcal{M}}|^2$ we only consider the $X(3872)$ meson interacting with D^0 and \bar{D}^{0*} (or \bar{D}^0 and D^{0*}) since the $X(3872)$ meson does not have its isospin partner. In Eq. (16), $|\vec{p}_i|$ and $|\vec{p}_f|$ represent the three-momenta of the initial and final particles in the center of mass frame. For coupling constants, we use $g_{\rho DD} = g_{\rho D^* D^*} = 2.52$, $g_{\psi DD} = g_{\psi D^* D^*} = 7.64$ from [18], and $g_{\pi D^* D} = 6.3$ from the decay width of D^* meson [44]. The strong-coupling constants for the $X(3872)$ meson have been taken from Table II in Ref. [43], and those are summarized in Table II.

TABLE II: The strong-coupling constants for the $X(3872)$ meson [43].

	$J^P = 1^+$	$J^P = 2^-$
$g_{X_J D^* D}$	3.5 ± 0.7 GeV	189 ± 36
$g_{X_J \psi \rho}$	0.14 ± 0.03	-0.29 ± 0.08 GeV $^{-1}$
$g'_{X_1 \psi \rho}$		0.28 ± 0.09 GeV $^{-1}$

In Fig. 2, we show the cross sections for the absorption of both a $X_1(3872)$ meson and a $X_2(3872)$ meson by pions and ρ mesons via processes $X\pi \rightarrow \bar{D}^* D^*$, $X\pi \rightarrow \bar{D} D$, $X\rho \rightarrow \bar{D}^* D$, $X\rho \rightarrow D\bar{D}$, and $X\rho \rightarrow D^* \bar{D}^*$ as functions of the total center-of-mass energy $s^{1/2}$ above the threshold energy $s_0^{1/2}$ of each process. We see in Fig. 2 (a) that there exists a peak near the threshold energy for the endothermic process $X_1\pi \rightarrow \bar{D}^* D^*$ ($s_0^{1/2} = 4013.96$ MeV), while the cross sections for the other exothermic processes $X_1\pi \rightarrow \bar{D} D$ ($s_0^{1/2} = 4009.72$ MeV), $X_1\rho \rightarrow \bar{D}^* D$, $X_1\rho \rightarrow D\bar{D}$, and $X_1\rho \rightarrow D^* \bar{D}^*$ ($s_0^{1/2} = 4647.17$ MeV) become infinite near the threshold. The same general behaviors as these can be found for the spin-2 $X(3872)$ meson in Fig. 2(b). For the endothermic process $X_2\pi \rightarrow \bar{D}^* D^*$, however, there is a gradual decrease after a strong rise near the threshold. It is also noticeable that there exists a sharp dip very near the threshold and a gradual increase and decrease afterwards for the exothermic processes $X_2\rho \rightarrow D\bar{D}$ and $X_2\rho \rightarrow D^* \bar{D}^*$, which is similar to that shown in Ref. [43] for the dissociation cross section of J/ψ into the open-charm meson

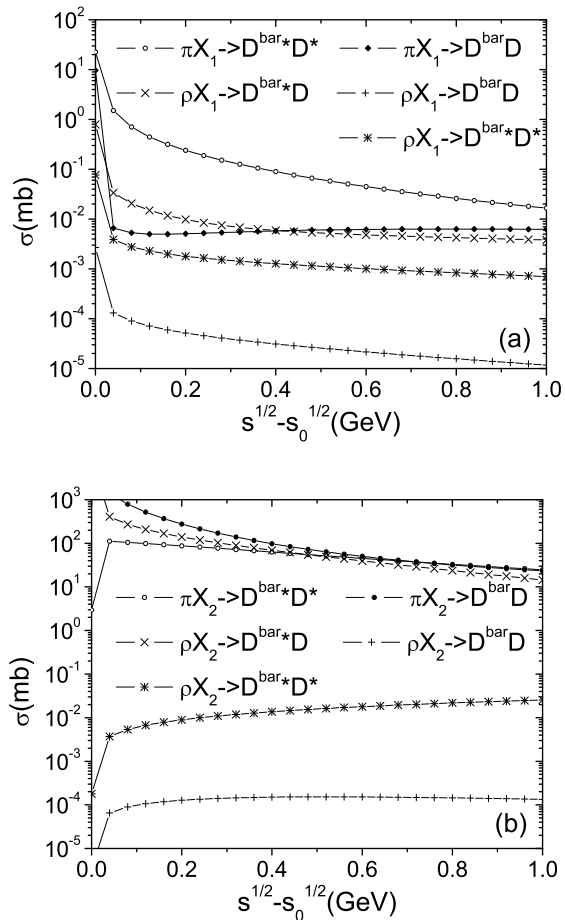


FIG. 2: Cross sections for the absorption of (a) a $X_1(3872)$ meson and (b) a $X_2(3872)$ meson by π and ρ mesons via processes $X\pi \rightarrow \bar{D}^*D^*$, $X\pi \rightarrow \bar{D}D$, $X\rho \rightarrow \bar{D}^*D$, $X\rho \rightarrow D\bar{D}$, and $X\rho \rightarrow D^*\bar{D}^*$.

mediated by the spin-2 $X(3872)$ meson. These differences are due to two different interaction mechanisms originating from two possible spin quantum numbers. The additional derivative in the interaction Lagrangian for the spin-2 $X(3872)$ meson causes the completely different energy dependence on the cross sections especially for the processes $X\rho \rightarrow D\bar{D}$ and $X\rho \rightarrow D^*\bar{D}^*$.

We also clearly see in Fig. 2 that the absorption cross sections for the processes $X\pi \rightarrow \bar{D}^*D^*$, $X\pi \rightarrow \bar{D}D$, and $X\rho \rightarrow \bar{D}^*D$ are much bigger when the spin of $X(3872)$ mesons is 2 than when it is 1. This is largely attributed to the large strong-coupling constant used to evaluate the cross sections for the processes having X_2D^*D interactions. For the processes involving the ρ meson, the additional derivative in the interaction Lagrangian for the spin-2 $X(3872)$ meson causes 10-40 times bigger cross sections in the processes $X_2\rho \rightarrow D\bar{D}$ and $X_2\rho \rightarrow D^*\bar{D}^*$ compared to those in the processes $X_1\rho \rightarrow D\bar{D}$ and

$X_1\rho \rightarrow D^*\bar{D}^*$ as shown in Fig. 2 when the strong couplings $g_{X_1\psi\rho}$, $g_{X_2\psi\rho}$, and $g'_{X_2\psi\rho}$ have been used. In the processes $X\pi \rightarrow \bar{D}^*D^*$, $X\pi \rightarrow \bar{D}D$, and $X\rho \rightarrow \bar{D}^*D$, however, the additional derivative brings out roughly $m_D \sim 1.9$ GeV. This factor will multiply the already large coupling constant $g_{X_2D^*D}$ given in Table II, making the effective coupling strength ($\sim 189 \times 1.9$ GeV) much larger compared to $g_{X_1D^*D} = 3.5$ GeV. This explains the bigger cross sections for the $X_2(3872)$ meson than those for the $X_1(3872)$ meson in Fig. 2.

Both strong coupling constants $g_{X_1D^*D}$ and $g_{X_2D^*D}$ were obtained from *one* experimental measurement using *two* different spin possibilities [43]. As was already pointed out, however, the analysis of the $X(3872)$ meson decaying to \bar{D}^0D^{*0} disfavors the 2^- quantum number because of the angular momentum barrier in its near-threshold decay [25, 26]. The D meson should have the relative angular momentum in order to be able to interact with the spin-2 $X(3872)$ meson to satisfy the angular momentum conservation. Therefore, the coupling constant $g_{X_2D^*D}$ has to be large to compensate for the angular momentum suppression near threshold.

Nevertheless, it is still possible to get a smaller strong coupling constant $g_{X_2D^*D}$ when the $X(3872)$ meson mass increases slightly. In Appendix A, we have investigated the origin of the big strong-coupling constant $g_{X_2D^*D}$, and have found that it is very sensitive to the variation of the $X(3872)$ meson mass. Varying the mass within the experimental uncertainty, we estimate that $g_{X_2D^*D}$ could be reduced by a factor of $\sqrt{3}$ and the cross sections of the spin-2 $X(3872)$ meson evaluated in Fig. 2 by a factor of 3.

The bigger cross sections for the spin-2 $X(3872)$ meson are contrary to naive expectations. It is expected that the size of the bag containing four quarks should be at least bigger than that of the bag having two quarks. In the simple bag model the size of the bag increases with the number of quarks inside the bag as $R \propto N_q^{1/4}$ [?]. Since the cross section depends on the size of the hadron in general, we expect the cross section of the $X(3872)$ meson composed of four quarks to be bigger than that of the $X(3872)$ meson made up of two quarks. However, we see here only the effects from the interaction mechanism caused by two different spins since the interaction Lagrangians are blind to the size of the $X(3872)$ meson.

IV. TIME EVOLUTION OF THE $X(3872)$ MESON ABUNDANCE IN HADRONIC MATTER

Using the cross sections evaluated in the previous section we now consider the time evolution of the $X(3872)$ meson abundance in hadronic matter. We build the evolution equation consisting of the densities and abundances for hadrons participating in all processes shown in Fig. 1: π , ρ , D^* , and D mesons.

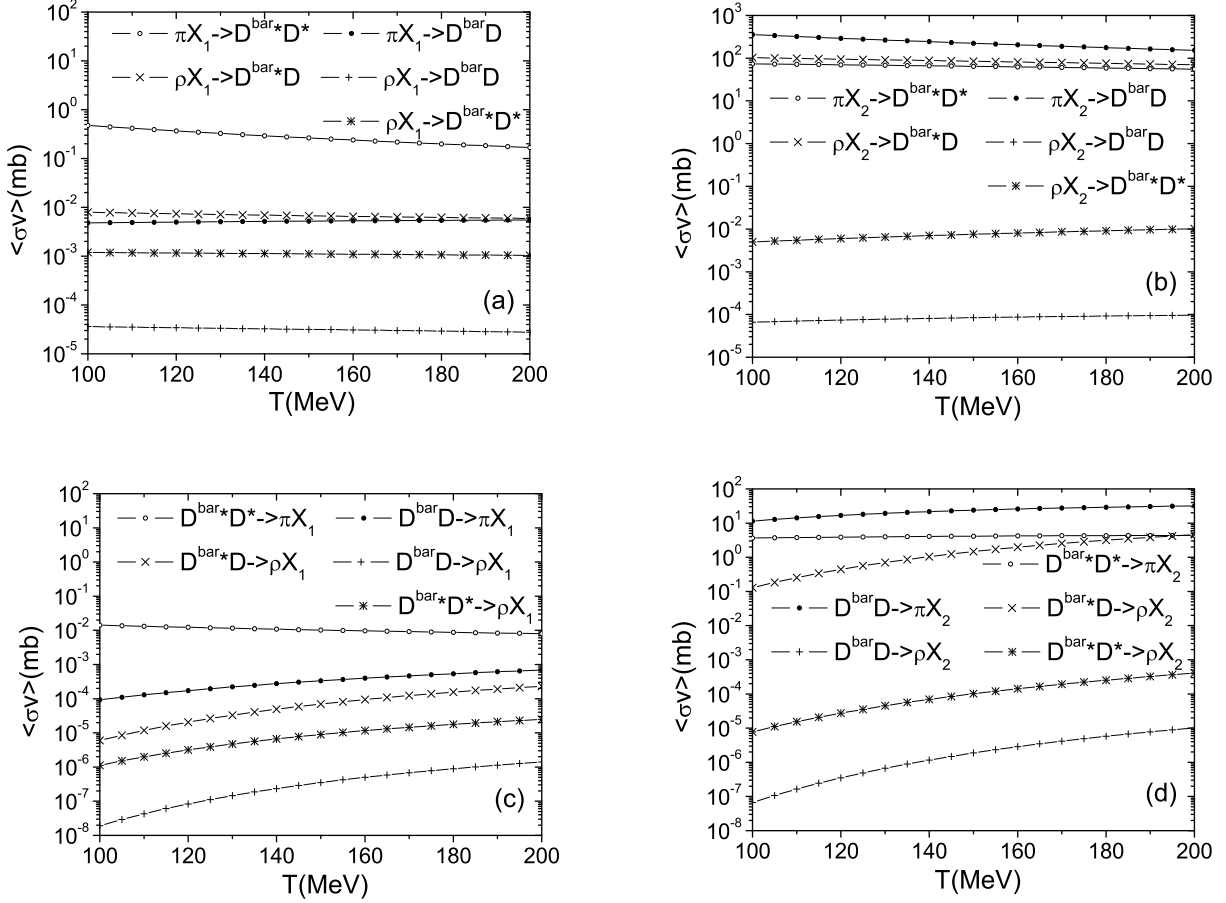


FIG. 3: Thermally averaged cross sections for the absorption of (a) a $X_1(3872)$ meson and (b) a $X_2(3872)$ meson by pions and ρ mesons via processes $X\pi \rightarrow \bar{D}^*D^*$, $X\pi \rightarrow \bar{D}D$, $X\rho \rightarrow \bar{D}^*D$, $X\rho \rightarrow D\bar{D}$, and $X\rho \rightarrow D^*\bar{D}^*$ and their inverse processes $\bar{D}^*D^* \rightarrow X\pi$, $\bar{D}D \rightarrow X\pi$, $\bar{D}^*D \rightarrow X\rho$, $D\bar{D} \rightarrow X\rho$, and $D^*\bar{D}^* \rightarrow X\rho$ for (c) a $X_1(3872)$ meson and (d) a $X_2(3872)$ meson.

$$\frac{dN_X(\tau)}{d\tau} = R_{QGP}(\tau) + \sum_{l,c,c'} \left(\langle\sigma_{cc' \rightarrow lX} v_{cc'}\rangle n_c(\tau) N_{c'}(\tau) - \langle\sigma_{lX \rightarrow cc'} v_{lX}\rangle n_l(\tau) N_X(\tau) \right), \quad (17)$$

where $n_l(\tau)$ and $n_c(\tau)$ are, respectively, the density of a light meson such as a pion or a ρ meson and the density of a charmed meson in the hadronic matter at proper time τ , whereas $N_{c'}(\tau)$ is the abundance of the other charmed meson in each process shown in Fig. 1 at proper time τ . $n_l(\tau)$, $n_c(\tau)$ and $N_{c'}(\tau)$ are calculated from Eq. (1) by assuming that light mesons and charmed mesons are in equilibrium and vary in time through the temperature profile introduced below, Eq. (19). In the above rate equation, Eq. (17), $\langle\sigma_{ab \rightarrow cd} v_{ab}\rangle$ is the cross section averaged over the thermal distribution for initial two particles in a two-body process $ab \rightarrow cd$ given by [46]

$$\begin{aligned} & \langle\sigma_{ab \rightarrow cd} v_{ab}\rangle \\ &= \frac{\int d^3\mathbf{p}_a d^3\mathbf{p}_b f_a(\mathbf{p}_a) f_b(\mathbf{p}_b) \sigma_{ab \rightarrow cd} v_{ab}}{\int d^3\mathbf{p}_a d^3\mathbf{p}_b f_a(\mathbf{p}_a) f_b(\mathbf{p}_b)} \\ &= \frac{1}{4\alpha_a^2 K_2(\alpha_a) \alpha_b^2 K_2(\alpha_b)} \int_{z_0}^{\infty} dz K_1(z) \sigma(s = z^2 T^2) \\ & \times [z^2 - (\alpha_a + \alpha_b)^2][z^2 - (\alpha_a - \alpha_b)^2], \quad (18) \end{aligned}$$

with $\alpha_i = m_i/T$, $z_0 = \max(\alpha_a + \alpha_b, \alpha_c + \alpha_d)$, K_1 and K_2 being the modified Bessel function of the first and second kind, respectively and v_{ab} denoting the relative velocity of the initial two interacting particles a and b , $v_{ab} = \sqrt{(p_a \cdot p_b)^2 - m_a^2 m_b^2} / (E_a E_b)$.

The $X(3872)$ meson abundance at proper time τ , $N_X(\tau)$, depends on both the dissociation rate such as $X\pi \rightarrow \bar{D}^*D^*$, $X\pi \rightarrow \bar{D}D$, $X\rho \rightarrow \bar{D}^*D$, $X\rho \rightarrow D\bar{D}$, and $X\rho \rightarrow D^*\bar{D}^*$ and the production rate through the inverse processes, $\bar{D}^*D^* \rightarrow X\pi$, $\bar{D}D \rightarrow X\pi$, $\bar{D}^*D \rightarrow X\rho$,

$D\bar{D} \rightarrow X\rho$, and $D^*\bar{D}^* \rightarrow X\rho$. We use the detailed balance relations based on the results for the forward processes shown in Fig. 2 in evaluating the thermally averaged cross sections of the inverse processes. The results are shown in Fig. 3.

In Eq. (17), $n_l(\tau)$, $n_c(\tau)$ and $N_{c'}(\tau)$ varies in time through the temperature profile developed to describe the dynamics of relativistic heavy ion collisions. We use the schematic model based on the boost invariant Bjorken picture with an accelerated transverse expansion [20, 47]. The system of the quark-gluon plasma of its final transverse size R_C at the chemical freeze-out time τ_C expands with its transverse velocity v_C and transverse acceleration a_C . The temperature of the system is maintained with a constant temperature T_C until the end of the mixed phase at τ_H , and decreases afterwards to the kinetic freeze-out temperature T_F . The volume and temperature profiles as a function of the proper time τ are as follows:

$$\begin{aligned} V(\tau) &= \pi[R_C + v_C(\tau - \tau_C) + a_C/2(\tau - \tau_C)^2]^2\tau_C, \\ T(\tau) &= T_C - (T_H - T_F)\left(\frac{\tau - \tau_H}{\tau_F - \tau_H}\right)^{4/5}, \end{aligned} \quad (19)$$

with T_H and τ_F being the hadronization temperature, and the freeze-out time, respectively. The values used in Eq. (19) are summarized in Table III.

TABLE III: Values for the volume and temperature profiles in the schematic model Eq. (19).

	Temp.(MeV)	Time (fm/c)
$R_C = 8.0$ fm	$T_C = 175$	$\tau_C = 5.0$
$v_C = 0.4c$	$T_H = 175$	$\tau_H = 7.5$
$a_C = 0.02c^2/\text{fm}$	$T_F = 125$	$\tau_F = 17.3$

In solving Eq. (17) we have assumed that the total number of charm quarks in charmed hadrons is conserved during the evolution of the hadronic matter. It has been discussed that chances for charmed mesons to be produced and destroyed in the hadronic matter are very small because of their small production and annihilation cross sections [18, 19, 48]. The light mesons are assumed to be in equilibrium with the medium and the total number of the pion is set to 926 at freeze-out [47] and that of the ρ meson to 68 after considering the contributions from the decays of resonances. To take into account the effect of the production of the $X(3872)$ meson through hadronization from the quark-gluon plasma, we include the term $R_{QGP}(\tau)$ [20] given by

$$R_{QGP}(\tau) = \begin{cases} N_X^0/(\tau_H - \tau_C), & \tau_C < \tau < \tau_H \\ 0, & \text{otherwise} \end{cases} \quad (20)$$

with N_X^0 being the total number of the $X(3872)$ meson in Table I produced from quark-gluon plasma either by the two-quark coalescence or by the four-quark coalescence. We assume here that the volume of the quark-gluon plasma decreases linearly during the phase-transition time $\tau_H - \tau_C = 2.5$ fm/c whereas that of the hadron gas increases with a rate enough to occupy both the decreased volume of the quark-gluon plasma and the newly increased volume of the entire system by the expansion.

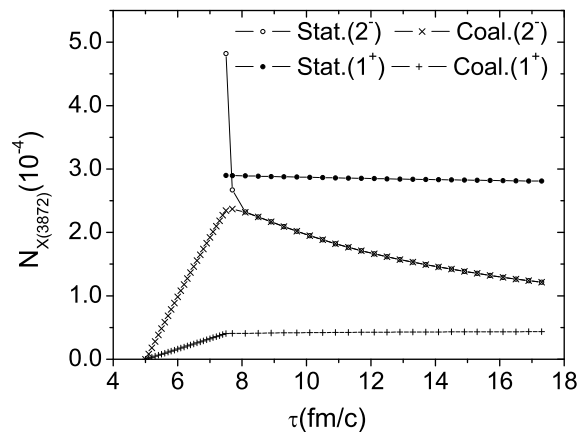


FIG. 4: Time evolution of $X(3872)$ meson abundances in central Au-Au collisions at $\sqrt{s_{NN}} = 200$ GeV for different states produced from the quark-gluon plasma.

In Fig. 4, we show the abundances of the $X(3872)$ meson as a function of the proper time for different states produced from the quark-gluon plasma in central Au-Au collisions at $\sqrt{s_{NN}} = 200$ GeV. Since the scattering cross sections for the 1^+ state $X_1(3872)$ meson are so small as shown in Fig. 2, the abundance obtained by the four-quark coalescence increases very slightly to 4.3×10^{-5} , while the expectation from the statistical model decreases also very slightly to 2.8×10^{-4} . However, due to the large scattering cross sections for the 2^- state $X(3872)$ meson, the $X(3872)$ meson in the normal $c\bar{c}$ state with d -wave has more chances to interact with light mesons in the hadronic evolution, and therefore the abundance decreases fast to 1.2×10^{-4} . The thermal model expectation for the spin-2 $X(3872)$ meson also decreases rapidly, follows the evolution of the coalescence model abundance, and evolves afterward together. The final ratio of the abundance for the $X_2(3872)$ meson over that for the $X_1(3872)$ meson both in the coalescence model is expected to be ~ 2.8 at the kinetic freeze-out.

Based on the above investigation about the time evolution of the $X(3872)$ meson, we can further consider the possibility of producing a hadronic molecular state of the spin-1 $X(3872)$ meson. If the state is a hadronic molecule composed of $D^0\bar{D}^{*0}(\bar{D}^0D^{*0})$ in s -wave, it will be dominantly produced at the end of the hadronic phase through

hadronic coalescence. The production in the hadronic phase through the two body hadronic interaction would be very small. For such process to be possible, the inverse processes like $\bar{D}^*D^* \rightarrow X\pi$, $\bar{D}D \rightarrow X\pi$, $\bar{D}^*D \rightarrow X\rho$, $D\bar{D} \rightarrow X\rho$, and $D^*\bar{D}^* \rightarrow X\rho$ should prevail the forward processes. We have already seen, however, in Fig. 3 that the thermally averaged cross sections of the inverse processes are smaller than those of the forward processes. However, this does not mean that the $X(3872)$ meson can not be produced in the hadronic phase. In fact, hadronic coalescence will continue to occur but the total absorption should be very large since the size of the loosely bound hadronic molecule is thought to be much bigger than that of the compact tetraquark state with the same spin.

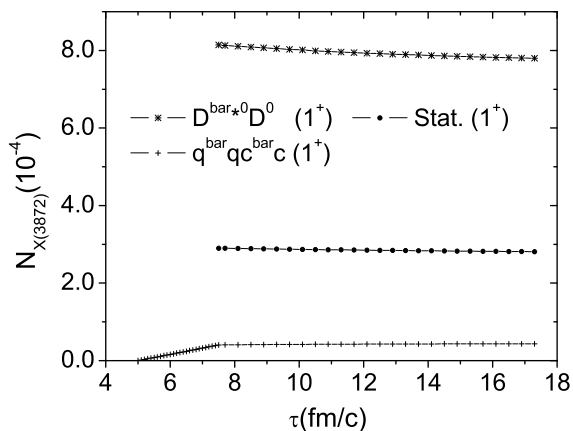


FIG. 5: The possible time evolution of the hadronic molecular state of the $X(3872)$ meson produced during the hadronic stage in central Au-Au collisions at $\sqrt{s_{NN}} = 200$ GeV when $X(3872)$ is assumed to be a 1^+ state.

With this in mind we can estimate the number of $X(3872)$ mesons in the hadronic phase by solving the rate equation, Eq. (17) for the hadronic molecular state backwards in time from the final yield of 7.8×10^{-4} [10, 11] calculated through the hadron coalescence at the end of the hadronic stage. As shown in Fig. 5, when the hadronic molecular state of the $X_1(3872)$ meson is produced sometime during the hadronic stage by the hadron coalescence, the number of $X(3872)$ mesons is expected to be in the range between 7.8×10^{-4} and 8.1×10^{-4} . Owing to the small cross sections evaluated in this work, which are blind to the size of the hadron, the yield decreases slightly during the hadronic stage, finally resulting to the ratio ~ 18 between the hadronic molecular state and the tetraquark state at the kinetic freeze-out.

The discussion on the production yield for a molecular state of the $X(3872)$ meson is based on the assumption that it is a $D^0\bar{D}^{*0}$ state. However, it has been shown that charged components of D and D^* mesons also play an essential role in explaining the branch-

ing ratio of the $X(3872)$ meson decaying to ω and ρ mesons [49–51]. If we take into account a linear combination of D and D^* mesons for the $X(3872)$ meson, $|X(3872)\rangle = 1/\sqrt{2}(|D^0\bar{D}^{*0}\rangle + |D^+D^{*-}\rangle)$, then we have to evaluate the average production yields coming from both $D^0\bar{D}^{*0}$ and D^+D^{*-} . Thus, the production yield would be the same since the numbers of D or D^* mesons are independent of their charges.

In this analysis, we have used the phenomenological model, Eq. (19), assuming the first order phase transition at hadronization, which is not a true situation in heavy ion collisions experiment at RHIC top energy. The transition is a crossover rather than a first order [5]. We do not expect, however, that taking the crossover phase transition into our consideration affects significantly the time evolution of $X(3872)$ meson abundance during the hadronic stage, since it has been initiated from the production yield at the hadronization temperature as shown in Fig. 4. We focus on the production of the $X(3872)$ meson from a quark-gluon plasma through coalescence during the crossover transition.

Assuming that the coalescence production of the $X(3872)$ meson continuously takes place at all temperatures during the crossover transition, we investigate the explicit temperature-dependent production of the $X(3872)$ meson using the coalescence formula obtained from the overlap between the density matrix of the constituents and the Wigner function of the $X(3872)$ meson. We note that the yield of the spin-2 $X(3872)$ meson by two-quark coalescence is $\propto T^2/(1+CT)^3$, whereas that of the spin-1 $X(3872)$ meson by four-quark coalescence is $\propto 1/(1+CT)^3$ with a same constant C [11]; as the temperature decreases, the production rate for the spin-1 $X(3872)$ meson increases but that of the spin-2 $X(3872)$ meson decreases. Hence, we find that the production of the $X(3872)$ meson through coalescence during the transition is also dependent on its spin. We expect the explicit temperature-dependent production rate of the $X(3872)$ meson, together with the changes in both the number of constituent quarks and the volume of the quark-gluon plasma participating in the production of $X(3872)$ mesons during the crossover transition, to modify the simple linear production of the $X(3872)$ meson in the first order transition shown in Fig. 4. The clear picture about hadron production during the crossover transition is currently not available and needs further study.

V. CONCLUSION

We have studied the hadronic effects on the $X(3872)$ meson abundance in heavy ion collisions using one meson exchange model with the effective Lagrangian. To take into account the effects due to two different spin possibilities of the $X(3872)$ meson, we have evaluated two absorption cross sections for both $J^P = 1^+$ and 2^- states of the $X(3872)$ meson by pions and rho mesons during the hadronic stage of heavy ion collisions. We have found

that the absorption cross sections and their thermal averages are strongly dependent on the structure and the quantum number of the $X(3872)$ meson; the energy dependence of the cross sections is quite different for two spin states as shown in Fig. 2, and the cross sections are much bigger for a 2^- state than those for a 1^+ state. Therefore, it is expected that the spin-2 $X(3872)$ meson can be absorbed by light mesons much more easily than the spin-1 $X(3872)$ meson.

We have further investigated the time evolution of the abundances for two possible quantum number states of the $X(3872)$ meson. We have found that the variation of the $X(3872)$ meson abundance during the expansion of the hadronic matter is also strongly affected by the quantum number of the $X(3872)$ meson; the $X_1(3872)$ meson abundance slightly changes to 4.3×10^{-5} , while the $X_2(3872)$ meson abundance varies significantly to 1.2×10^{-4} , leading to the final abundance ratio ~ 2.8 between $X_2(3872)$ and $X_1(3872)$ mesons at the kinetic freeze-out. We therefore suggest that studying the abundance of the $X(3872)$ meson in relativistic heavy ion collisions provides a chance to infer its quantum number as well as its structure.

We have also considered the hadronic molecular state $D^0 \bar{D}^{*0} (\bar{D}^0 D^{*0})$ possibly produced from $D^0 (\bar{D}^0)$ and $\bar{D}^{*0} (D^{*0})$ sometime during the hadronic stage. The abundance is expected to be in the range between 7.8×10^{-4} and 8.1×10^{-4} , resulting in the final ratio ~ 18 between the hadronic molecular state and the tetraquark state.

In the present experiment at STAR, open charm mesons are reconstructed from their hadronic decay products [52]. However, a heavy flavor tracker, which will make the reconstruction of the secondary vertex of open charm mesons possible, is scheduled to operate in the near future. Then we are able to find charmed mesons purely coming from the $X(3872)$ mesons ($X \rightarrow D^0 \bar{D}^{*0}$ or $X \rightarrow D^0 \bar{D}^0 \pi$ [31]) and measure the yield of $X(3872)$ mesons produced by the coalescence in heavy ion collisions. The possibility of the $X(3872)$ meson production from the B meson decay is very low at RHIC top energy. The estimation on the time evolution of the $X(3872)$ meson abundance shows that when the number of D mesons observed through the vertex detector is cumulated to be about 10^4 , at least a few $X(3872)$ mesons are expected to be produced if the $X(3872)$ meson is in a hadronic molecule state. If we need to collect one order of magnitude larger numbers of D mesons to obtain a trace for a $X(3872)$ meson, we can conclude that we are finding a $X(3872)$ meson in a tetraquark state. Therefore, a factor of 18 smaller yield for the $X(3872)$ meson in a tetraquark state is enough to be used to discriminate the structure of the spin-1 $X(3872)$ meson.

Acknowledgements

This work was supported by the Korea National Research Foundation under Grants No. KRF-2011-0020333 and No. KRF-2011-0030621 and the Korean Ministry of Education through the BK21 program.

Appendix A: Dependence of the strong coupling constants on the $X(3872)$ meson mass

In order to understand the origin of the big difference between $g_{X_1 D^* D}$ and $g_{X_2 D^* D}$ we investigate the relation between two strong-coupling constants. We simply consider the decay rate of the $X(3872)$ meson decaying to D^0 and \bar{D}^{*0} ,

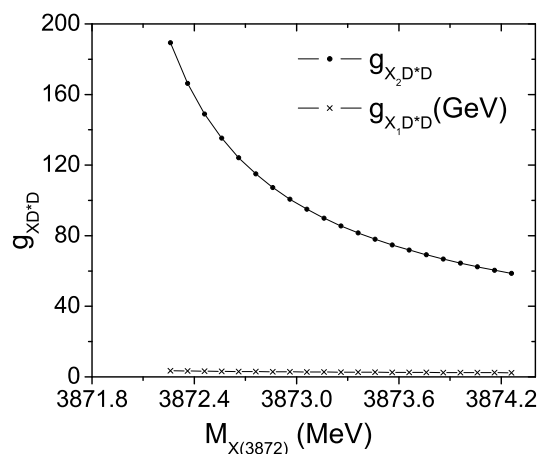


FIG. 6: The strong coupling constants $g_{X_1 D^* D}$ and $g_{X_2 D^* D}$ as functions of the $X(3872)$ meson mass.

$$d\Gamma(X \rightarrow D^0 \bar{D}^{*0}) = \frac{1}{2s_X + 1} \frac{(2\pi)^4}{2m_X} \sum_{pol} |\mathcal{M}|^2 d\Phi_2(k; p, q), \quad (\text{A1})$$

where $d\Phi_2(k; p, q)$ is the element of the two-body phase-space density given by

$$d\Phi_2(k; p, q) = \delta^4(k - p - q) \frac{d^3 p}{(2\pi)^3 2E_{D^0}} \frac{d^3 q}{(2\pi)^3 2E_{\bar{D}^{*0}}}. \quad (\text{A2})$$

In the rest frame of the $X(3872)$ meson, the decay rate Eq. (A1) becomes,

$$\Gamma(X \rightarrow D^0 \bar{D}^{*0}) = \frac{1}{8\pi} \frac{1}{m_X^2} |\vec{p}| \frac{1}{2s_X + 1} \sum_{pol} |\mathcal{M}|^2 \quad (\text{A3})$$

with

$$|\vec{p}| = \frac{\sqrt{(m_X^2 - (m_{D^0} - m_{\bar{D}^{*0}})^2)(m_X^2 - (m_{D^0} + m_{\bar{D}^{*0}})^2)}}{2m_X}. \quad (\text{A4})$$

Since we consider *two* spin possibilities for the $X(3872)$ meson to explain *one* experimental observation, we obtain the following condition using the interaction Lagrangians, Eq. (4),

$$\begin{aligned} & \frac{1}{3} \sum_{pol} |g_{X_1 D^* D} \epsilon^\mu(k) \epsilon_\mu^*(q)|^2 \\ &= \frac{1}{5} \sum_{pol} |g_{X_2 D^* D} \pi^{\mu\nu}(k) \epsilon_\mu^*(q) p_\nu|^2, \end{aligned} \quad (\text{A5})$$

by requiring $\Gamma_{X_2} = \Gamma_{X_1}$. This condition is responsible for the difference between $g_{X_1 D^* D} = 3.5$ GeV and $g_{X_2 D^* D} = 189$ when a mass of the $X(3872)$ meson is 3872.26 MeV. We can obtain, using Eq. (A5), the other strong coupling constant of the $X(3872)$ meson when one of them is known.

We have also found that $g_{X_2 D^* D}$ is sensitive to the variation of the $X(3872)$ meson mass when obtaining it from the requirement $\Gamma_{X_2} = \Gamma_{X_1}$. Since we know that a recent measurement of the $X(3872)$ meson mass from its decay mode, $X \rightarrow D^{*0} \bar{D}^0$ is 3872.9 MeV [27], we vary the mass of the $X(3872)$ meson, and see how the strong coupling constants $g_{X_1 D^* D}$ and $g_{X_2 D^* D}$ change.

As shown in Fig. 6, $g_{X_2 D^* D}$ decreases from 189 to 107 whereas $g_{X_1 D^* D}$ changes from 3.5 GeV to 2.5 GeV when the mass of the $X(3872)$ meson increases from 3872.3 MeV to 3872.9 MeV. We expect the above new strong coupling constants obtained when the mass of the $X(3872)$ meson is 3872.9 MeV to reduce the cross sections evaluated in Sec. III by a factor of 3 for the $X_2(3872)$ meson, and by a factor of 2 for the $X_1(3872)$ meson, respectively.

Appendix B: Hadronic effects on the $X(3872)$ meson by baryons

In this appendix, we consider a system of baryons interacting with $X(3872)$ mesons to describe the hadronic effects on the $X(3872)$ meson more realistically. As we find that the cross sections of the $X(3872)$ meson with different spin states strongly depend on the strength of the strong coupling-constants, we expect the hadronic effects on $X(3872)$ mesons by baryons also lead to similar results as shown in Sec. III.

Since the most abundant baryons available in the system are nucleons, we take the absorption of $X(3872)$ mesons by nucleons into consideration: $XN \rightarrow \bar{D}^* \Lambda_C$ and $XN \rightarrow \bar{D} \Lambda_C$.

In addition to the interaction Lagrangians introduced in Eq. (3), we need the following additional interaction Lagrangians to describe the diagrams shown in Fig. 7:

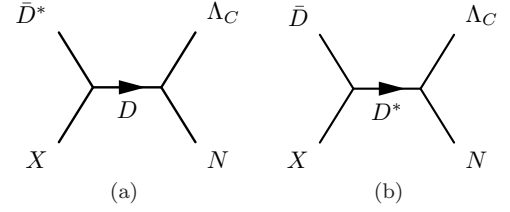


FIG. 7: Born diagrams for the $X(3872)$ meson absorption by nucleons; $XN \rightarrow \bar{D}^* \Lambda_C$ (a) and $XN \rightarrow \bar{D} \Lambda_C$ (b).

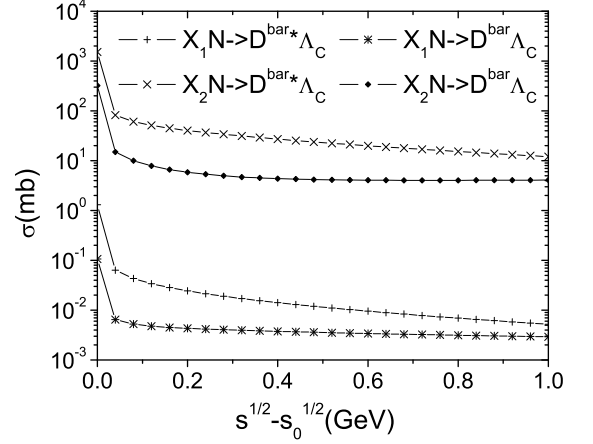


FIG. 8: Cross sections for the absorption of $X(3872)$ mesons with different spin states by nucleon via reactions, $XN \rightarrow \bar{D}^* \Lambda_C$ and $XN \rightarrow \bar{D} \Lambda_C$.

$$\begin{aligned} \mathcal{L}_{D^* N \Lambda_C} &= g_{D^* N \Lambda_C} (\bar{N} \gamma_\mu \Lambda_C \bar{D}^{*\mu} + D^{*\mu} \bar{\Lambda}_C \gamma_\mu N), \\ \mathcal{L}_{D N \Lambda_C} &= i g_{D N \Lambda_C} (\bar{N} \gamma_5 \Lambda_C \bar{D} + D \bar{\Lambda}_C \gamma_5 N), \end{aligned} \quad (\text{B1})$$

with coupling constants $g_{D^* N \Lambda_C} = -5.6$ and $g_{D N \Lambda_C} = 13.5$ [53]. Using these interaction Lagrangians we easily obtain the amplitudes for the reaction, $XN \rightarrow \bar{D}^* \Lambda_C$,

$$\begin{aligned} \mathcal{M}_{X_1 N \rightarrow \bar{D}^* \Lambda_C} &= -i g_{D N \Lambda_C} g_{X_1 D^* D} \epsilon_1^\mu \epsilon_{3\mu}^* \frac{1}{t - m_D^2} \\ &\quad \times \bar{\Lambda}_C(p_4) \gamma_5 N(p_2), \\ \mathcal{M}_{X_2 N \rightarrow \bar{D}^* \Lambda_C} &= -i g_{D N \Lambda_C} g_{X_2 D^* D} \pi_1^{\mu\alpha} \epsilon_2^{*\mu} (p_1 - p_3)_\alpha \\ &\quad \times \frac{1}{t - m_D^2} \bar{\Lambda}_C(p_4) \gamma_5 N(p_2). \end{aligned} \quad (\text{B2})$$

for both spin-1 and spin-2 $X(3872)$ meson states. Similarly, we get the amplitudes,

$$\begin{aligned} \mathcal{M}_{X_1 N \rightarrow \bar{D} \Lambda_C} &= -g_{D^* N \Lambda_C} g_{X_1 D^* D} \epsilon_1^\mu \frac{1}{t - m_D^{*2}} \\ &\quad \times \left(-g_{\mu\nu} + \frac{(p_1 - p_3)_\mu (p_1 - p_3)_\nu}{m_D^{*2}} \right) \bar{\Lambda}_C(p_4) \gamma^\nu N(p_2), \end{aligned}$$

$$\begin{aligned} \mathcal{M}_{X_2 N \rightarrow \bar{D} \Lambda_C} &= -g_{D^* N \Lambda_C} g_{X_2 D^* D} \pi_1^{\mu\alpha} p_{3\alpha} \frac{1}{t - m_D^{*2}} \\ &\times \left(-g_{\mu\nu} + \frac{(p_1 - p_3)_\mu (p_1 - p_3)_\nu}{m_D^{*2}} \right) \bar{\Lambda}_C(p_4) \gamma^\nu N(p_2). \end{aligned} \quad (\text{B3})$$

for the reaction $XN \rightarrow \bar{D}\Lambda_C$.

We show in Fig. 8 the final isospin- and spin-averaged cross sections, (16) for the above reactions. We see that cross sections for the spin-1 $X(3872)$ meson are again much larger than those for the spin-2 $X(3872)$ meson due to the same reasons discussed in Sec. III. When compared to absorption cross sections by pions or rho mesons shown in Fig. 2, absorption cross sections by nucleons for spin-1 $X(3872)$ mesons are smaller than that of the process, $X_1\pi \rightarrow \bar{D}^*D^*$, much larger than that for the reaction $X_1\rho \rightarrow D^*\bar{D}^*$ which contains a three-vector meson interaction vertex, but similar in size to other cross

sections. For spin-2 $X(3872)$ mesons, absorption cross sections by nucleons are smaller than those by pions, but much larger than cross sections by rho meson for reactions, $X_2\rho \rightarrow D\bar{D}$ and $X_2\rho \rightarrow D^*\bar{D}^*$.

We therefore expect that including hadronic effects on the $X(3872)$ meson by nucleons accelerates the variation of the $X(3872)$ meson abundance during the hadronic stage of heavy ion collisions. However, because the yield of nucleons is smaller than that of pions by a factor of 10 in the statistical model, the chance for the $X(3872)$ meson to interact with nucleons is small and, as a result, hadronic effects on the $X(3872)$ meson by nucleons would not be dominant. In conclusion, the baryonic effects on the $X(3872)$ meson is comparable to mesonic effects but their contribution to the $X(3872)$ meson abundance change in the hadronic medium would be small due to the smaller yield compared to that of mesons.

-
- [1] I. Arsene *et al.* (BRAHMS Collaboration), Nucl. Phys. A **757**, 1 (2005).
[2] B. B. Back *et al.* (PHOBOS Collaboration), Nucl. Phys. A **757**, 28 (2005).
[3] J. Adams *et al.* (STAR Collaboration), Nucl. Phys. A **757**, 102 (2005).
[4] K. Adcox *et al.* (PHENIX Collaboration), Nucl. Phys. A **757**, 184 (2005).
[5] M. Gyulassy and L. McLerran, Nucl. Phys. A **750**, 30 (2005).
[6] S. Gupta, X. Luo, B. Mohanty, H. G. Ritter and N. Xu, Science, **332**, 1525 (2011).
[7] B. I. Abelev *et al.* (STAR Collaboration), Science, **328**, 58 (2010).
[8] H. Agakishiev *et al.* (STAR Collaboration), Nature, **473**, 353 (2011).
[9] N. Shah (STAR Collaboration), Acta Phys. Polon. Supp. **5**, 593 (2012).
[10] S. Cho *et al.* (ExHIC Collaboration), Phys. Rev. Lett. **106**, 212001 (2011).
[11] S. Cho *et al.* (ExHIC Collaboration), Phys. Rev. C **84**, 064910 (2011).
[12] A. Andronic, P. Braun-Munzinger, J. Stachel and H. Stocker, Phys. Lett. B **697**, 203 (2011).
[13] J. Cleymans, S. Kabana, I. Kraus, H. Oeschler, K. Redlich and N. Sharma, Phys. Rev. C **84**, 054916 (2011).
[14] L. Xue, Y. G. Ma, J. H. Chen and S. Zhang, Phys. Rev. C **85**, 064912 (2012).
[15] J. Steinheimer, K. Gudima, A. Botvina, I. Mishustin, M. Bleicher and H. Stocker, Phys. Lett. B **714**, 85 (2012).
[16] Sergei G. Matinyan and Berndt Muller, Phys. Rev. C **58**, 2994 (1998).
[17] Kevin L. Haglin, Phys. Rev. C **61**, 031902(R) (2000).
[18] Ziwei Lin and C. M. Ko, Phys. Rev. C **62**, 034903 (2000).
[19] Yongseok Oh, Taesoo Song, and Su Hounng Lee, Phys. Rev. C **63**, 034901 (2001).
[20] L. W. Chen, C. M. Ko, W. Liu, and M. Nielsen, Phys. Rev. C **76**, 014906 (2007).
[21] S. K. Choi *et al.* (Belle Collaboration), Phys. Rev. Lett. **91**, 262001 (2003).
[22] D. Acosta *et al.* (CDF Collaboration), Phys. Rev. Lett. **93**, 072001 (2004).
[23] V. M. Abazov *et al.* (D0 Collaboration), Phys. Rev. Lett. **93**, 162002 (2004).
[24] B. Aubert *et al.* (BABAR Collaboration), Phys. Rev. D **71**, 071103 (2005).
[25] G. Gokhroo *et al.* (Belle Collaboration), Phys. Rev. Lett. **97**, 162002 (2006).
[26] B. Aubert *et al.* (BABAR Collaboration), Phys. Rev. D **77**, 011102(R) (2008).
[27] T. Aushev *et al.* (Belle Collaboration), Phys. Rev. D **81**, 031103(R) (2010).
[28] B. Aubert *et al.* (BABAR Collaboration), Phys. Rev. D **82**, 011101(R) (2008).
[29] B. Aubert *et al.* (BABAR Collaboration), Phys. Rev. D **74**, 071101(R) (2006).
[30] B. Aubert *et al.* (BABAR Collaboration), Phys. Rev. Lett. **102**, 132001 (2009).
[31] J. Beringer *et al.* (Particle Data Group Collaboration), Phys. Rev. D **86**, 010001 (2012).
[32] M. Nielsen, F. S. Navarra and S. H. Lee, Phys. Rep. **497**, 41 (2010).
[33] A. Abulencia *et al.* (CDF Collaboration), Phys. Rev. Lett. **98**, 132002 (2007).
[34] P. Braun-Munzinger, J. Stachel, J. P. Wessels and N. Xu, Phys. Lett. B **344**, 43 (1995).
[35] P. Braun-Munzinger, J. Stachel, J. P. Wessels and N. Xu, Phys. Lett. B **365**, 1 (1996).
[36] P. Braun-Munzinger, I. Heppe and J. Stachel, Phys. Lett. B **465**, 15 (1999).
[37] P. Braun-Munzinger, D. Magestro, K. Redlich and J. Stachel, Phys. Lett. B **518**, 41 (2001).
[38] V. Greco, C. M. Ko, and P. Levai, Phys. Rev. Lett. **90**, 202302 (2003).
[39] V. Greco, C. M. Ko, and P. Levai, Phys. Rev. C **68**, 034904 (2003).
[40] R. J. Fries, B. Muller, C. Nonaka, and S. A. Bass, Phys. Rev. Lett. **90**, 202303 (2003).

- [41] R. J. Fries, B. Muller, C. Nonaka, and S. A. Bass, Phys. Rev. C **68**, 044902 (2003).
- [42] D. Molnar and S. A. Voloshin, Phys. Rev. Lett. **91**, 092301 (2003).
- [43] F. Brazzi, B. Grinstein, F. Piccinini, A. D. Polosa, and C. Sabelli, Phys. Rev. D **84**, 014003 (2011).
- [44] S. Ahmed *et al.* (CLEO Collaboration), Phys. Rev. Lett. **87**, 251801 (2001).
- [45] S. H. Lee and S. Cho, Few-Body Syst. **54**, 151 (2013).
- [46] P. Koch, B. Muller and J. Rafelski, Phys. Rep. **142**, 167 (1986).
- [47] Lie-Wen Chen, V. Greco, C. M. Ko, S. H. Lee, and W. Liu, Phys. Lett. B **601**, 34 (2004).
- [48] Z.-W. Lin, C. M. Ko, and B. Zhang, Phys. Rev. C **61**, 024904 (2000).
- [49] D. Gamermann and E. Oset, Phys. Rev. D **80**, 014003 (2009).
- [50] D. Gamermann, J. Nieves, E. Oset, and E. Ruiz Arriola, Phys. Rev. D **81**, 014029 (2010).
- [51] F. Aceti, R. Molina, and E. Oset, Phys. Rev. D **86**, 113007 (2012).
- [52] D. Tlusty (STAR Collaboration), Nucl. Phys. A **904-905**, 639c (2013).
- [53] W. Liu, C. M. Ko and Z. W. Lin, Phys. Rev. C **65**, 015203 (2001).